Publié par :
Published by:
Publicación de la:

Faculté des sciences de l'administration
2325, rue de la Terrasse
Pavillon Palasis-Prince, Université Laval
Québec (Québec) Canada G1V 0A6
Tél. Ph. Tel. : (418) 656-3644
Télec. Fax : (418) 656-7047

Disponible sur Internet :
Available on Internet
Disponible por Internet :

http://www4.fsa.ulaval.ca/la-recherche/publications/documents-de-travail/

DOCUMENT DE TRAVAIL 2018-001

Improved Home Deliveries in Congested Areas
Using Geospatial Technology

Khaled BELHASSINE
Leandro C. COELHO
Jacques RENAUD
Jean-Philippe GAGLIARDI

Document de travail également publié par le Centre interuniversitaire de recherche sur les réseaux d'entreprise, la logistique et le transport, sous le numéro CIRRELT-2018-02

Janvier 2018

Dépôt legal – Bibliothèque et Archives nationales du Québec, 2018
Bibliothèque et Archives Canada, 2018

ISBN 978-2-89524-458-5 (PDF)

Improved home deliveries in congested areas using geospatial technology

Khaled Belhassine[1,3], **Leandro C. Coelho**[1,2,3,4], **Jacques Renaud**[1,2,3,*], **Jean-Philippe Gagliardi**[5]

[1] Centre d'innovation en logistique et chaîne d'approvisionnement durables (CILCAD), Université Laval, Québec, Canada, G1V 0A6
[2] Department of Operations and Decision Systems, Université Laval, 2325, rue de la Terrasse, Québec, Canada, G1V 0A6
[3] Interuniversity Research Centre on Enterprise Networks, Logistics and Transportation (CIRRELT)
[4] Canada Research Chair in Integrated logistics, Université Laval, 2325, rue de la Terrasse, Québec, Canada, G1V 0A6
[5] Logix Operations, 951, rue de l'Etna, Québec, Canada, G3K 0B9

*Corresponding author: jacques.renaud@fsa.ulaval.ca

ABSTRACT

In this paper we introduce and empirically validate a methodology to transform geolocation observations of thousands of home delivery trips of an industrial partner into congestion data on segments of a road network. We describe the geomatics steps and algorithms required to associate each observation to the right road segment. From this data, we develop daily congestion index calendars as a function of the time of the day. The sectorial congestion ratios are developed to guide the delivery decisions of our partner. These data also make it possible to calculate the duration of a vehicle delivery tour by considering the congestion of each segment at the moment when it will be crossed. Using historical data of our partner, we demonstrate the accuracy of the developed procedures. Afterwards, we analyze the best departure times for delivery tours taking into account congestion. We show that by optimizing the tour departure times to avoid congestion enables a significant reduction of the tour duration by 22% and savings on CO_2 *equivalent* emissions of up to 43 tons per year for our industrial partner.

Keywords: Geolocation, geospatial technology, GPS, vehicle routing, traffic, congestion, CO_2 *e* emissions

Acknowledgments: This research was partly supported by grants 2014-05764 and 017633 from the Natural Sciences and Engineering Research Council of Canada (NSERC) and by the Centre d'Innovation en Logistique et Chaîne d'Approvisionnement Durable (CILCAD). The CILCAD receives financial support from the Green Fund under Priority 15.2 of the 2013-2020 Action Plan on Climate Change, a priority implemented by Transition Énergétique Québec (TEQ). We also thank Logix Operations Inc. and an important wholesaler partner in Quebec City for providing us with real data. This support is highly appreciated.

1. Introduction

Congestion arises in most roads and highways in major cities around the world. It can cause a significant variation in travel times, especially during peak hours, and thus have an impact on fuel consumption and, consequently, on greenhouse gas (GHG) emissions. For companies offering home delivery services, delays due to congestion directly affects the quality of the customer's experience and their costs. Companies offering home delivery and installation must therefore consider the risk of congestion when creating delivery schedules to be proposed to drivers and customers. Poor scheduling of visit times requiring customers to wait for the delivery of their product incurs a negative perception on the quality of service.

In this paper, we investigate how the use of geospatial technology to derive congestion factors throughout the day can improve delivery route planning for a major appliance and electronics retailer. To do this, we describe a methodological approach to perform a massive data analysis on the geolocation points (GPS) associated with the trips of the trucks of our partner. This allows us to derive a personalized mapping of the traffic it faces in its delivery areas. Advanced geomatics analyses are described to map GPS observations into the road network, deducing routes and the congestion rates on the road. These analyses allow us to evaluate the congestion faced by our partner's fleet and determine the best possible departure times. Savings are estimated in terms of time, salary and GHG emissions.

The *vehicle routing problem* (VRP) and its generalizations are extensively studied in the literature (Laporte 2009, Coelho et al., 2014, Koç et al., 2016, Ritzinger et al. 2016). Research on these practical problems has been greatly influenced by computer and technological innovations. During the 1990s, increased computing capacity led to the development of high-performance solution methods such as tabu search, genetic algorithms, and advanced neighborhood search algorithms (Gendreau et al., 2002, Cordeau et al., 2005, Potvin, 2009). Later, the availability of communication technology allowed the interaction between the dispatchers and the drivers, which led to the development of dynamic vehicle routing problems (DVRP) (Ichoua et al. 2006, Pillac et al., 2013). Today, the extensive use of electronic devices, the democratization of smart phones enabling the acquisition of geolocation data and the big data analysis make it possible to obtain real-time information on road congestion. The availability of this information has pushed the development of research into new types of problems (Sperenza, 2018).

These include *time-dependent vehicle routing problems* (TDVRPs) (Kok et al., 2012, Gendreau et al., 2015) and *pollution routing problems* (PRPs) that seek to optimize routing while considering GHG emissions (Bektas & Laporte, 2011).

These recent developments are just beginning to appear in commercial software (ORMS Today, 2016). In addition to technical difficulties involved in solving such problems, the lack of reliable and usable data on road congestion still complicates the time-dependent routing. In this article we present a complete and validated methodology that allows GPS data to be extracted and to deduce relevant congestion information and to use them in order to plan departure times and study the delivery sectors of our partner.

The remainder of this paper is organized as follows. In Section 2, we describe distribution problems appearing in the furniture and electronics industry as is the case of our industrial partner. Section 3 describes the main methodological processes associated with converting raw GPS observations into useful and insightful congestion information. The detailed analysis of a case study is presented in Section 4, followed by our conclusions in Section 5.

2. Vehicle routing in the furniture and electronics delivery industry

This project was carried out in close collaboration with one of the largest retailers in the field of electronics and appliances in Quebec. In order to offer a distinctive and high quality service, our partner offers a personalized delivery service performed by its own fleet of vehicles, drivers and assemblers/installers. The logistics process works as follows. When a customer makes a purchase, he has the option of selecting a set of days when the delivery can be made. In some cases, the customer may also require desired delivery time windows. Every evening, a computer system compiles the deliveries to be made for the next day and optimizes the routes. When the planning is complete, the system automatically generates a delivery confirmation for all customers, specifying whether their delivery will take place in the morning or afternoon. Overnight, order assembly and loading operations are performed at the distribution center and trucks are ready to start their trip by seven in the morning. With the evolution of deliveries, an automated phone system informs the customer of the imminence of the truck arrival.

Delivery planning is a complex process that must take into account the weight and volume of products, the location of customers, the required installation times as well as constraints related to vehicle characteristics. Depending on the level of quality or prestige associated with a specific product, additional constraints may influence the choice of installers and vehicles (Gagliardi et al., 2013). Finally, since drivers and installers are employees of the company, scheduling must consider lunch breaks and other regulations, adding an extra level of complexity as demonstrated in Coelho et al. (2016).

Our partner uses a home-based delivery planning software based on an evolved version of that proposed by Gagliardi et al. (2013). This in-house development offers the advantage of complete customization and full access to all data structure. This customization will make it possible to integrate the processing of the geolocation data as well as the calculation of the hourly congestion. These procedures are presented in the next section.

3. Geomatics data processing

In this section, we present the required steps to collect data, analyze them and extract useful information about traffic congestion for different time intervals for each day of the week. The methodology for calculating the travel time of a given route is also described.

3.1 Data acquisition

The first step is to perform the daily acquisition of GPS data from our partner. This data transfer is done automatically every night using a Python command (script) file. On average, 45,000 GPS points are transferred daily to a PostgreSQL/PostGIS geospatial database management system. Such a system coupled with the Quantum GIS software can save, analyze and visualize geospatial data. Each registered GPS point has several attributes, including: the route ID, the speed of the vehicle, the type of recording equipment used, the exact date and time of recording points, and the latitude/longitude coordinates. In our case, the average time between two consecutive recordings is 15 seconds.

3.2 Processing datasets

Once the raw data is imported, several treatments are performed to improve its quality. Initially, points with aberrant speeds (negative or greater than 150 km/h) are eliminated, as are points whose distance from the road network exceeds a certain limit (such as those recorded within buildings, parking lots, badges traversing a river, etc.). This limit varies depending on the recording equipment used. In the case of personal digital assistant (PDA-type) equipment, a point will be considered aberrant if it deviates more than 25 meters from a road section. For electronic logging devices (ELDs), which are much more accurate, the threshold is set to 15 meters. Subsequently, the aggregates of points recorded during a long downtime are deleted (delivery to a customer, refueling at a service station, loading of goods in a depot, etc.), in order to avoid affecting the calculation of average speeds and congestion. To be considered as an aggregate, GPS points must have a speed of less than 20 km/h and we must observe at least 12 observations within a 20-meter radius.

3.3 Assigning GPS points to road segments

Assigning the GPS points to their corresponding road segments is a process known as *Map Matching* (MM) (Quddus et al., 2007). There are four groups of MM approaches, including topological (White et al., 2000; Greenfeld, 2002; Quddus et al., 2003), probabilistic (Ochieng et al., 2004) advanced (Li and Chen, 2005; Wang et al., 2006), and geometric (Bernstein and Kornhauser, 1996), and each has its advantages and disadvantages.

The topological map-matching (tMM) algorithms consider information of heading, proximity, link connectivity and turn-restriction weights. Weight-based tMM algorithms are most robust and widely used (Greenfeld, 2002). Quddus et al. (2003) propose an enhancement of the topological map-matching algorithm. The probabilistic algorithm was first introduced by Honey et al. (1989). It requires the definition of an elliptical or rectangular confidence region around a position fix obtained from a navigation sensor. Ochieng et al. (2004) developed an enhanced probabilistic map-matching algorithm.

Advanced map-matching algorithms consider more refined concepts such as a Kalmam Filter or an Extended Kalman Filter (Li and Chen, 2005; Wang et al., 2006). It requires much more input data than geometric and topological algorithms. Thereby, this result in slower matching times and higher hardware workload.

The geometric MM method is based on the geometric relationship between GPS points and the road network. It does not consider the way links are connected to each other. For example, the *point-to-curve* technique (Bernstein and Kornhauser, 1996) assigns GPS points to the nearest road segment. Thus, the distance between each GPS point and each road segment is calculated and the segment for which the distance is minimal is selected. This method often produces incorrect results, especially on a dense urban networks and/or when the quality of the GPS signal is weak (White et al., 2000). Indeed, the nearest segment is not always the segment traveled. In Figure 1, the vehicle's trip is represented by the red line and points P^1 through P^5 have been recorded from a GPS device. The application of the *point-to-curve* technique would incorrectly assign point P^3 to the road segment on the left. In order to avoid these errors, we propose an algorithm that determines for each trip the segments actually traveled by the vehicle by recreating its full path. We then assign the GPS points to the nearest segments of the identified path. The steps of this algorithm are described next.

Figure 1. Incorrect assignment of point P^3 under the point-to-curve technique

Identifying each route direction

As a first step, we need to find each route direction by using the date and time of the GPS points. For a given trip all GPS points are connected from first to last. This step uses the time of each recorded point to determine the direction of movement of each vehicle and therefore to identify the departure and arrival points (Figure 2).

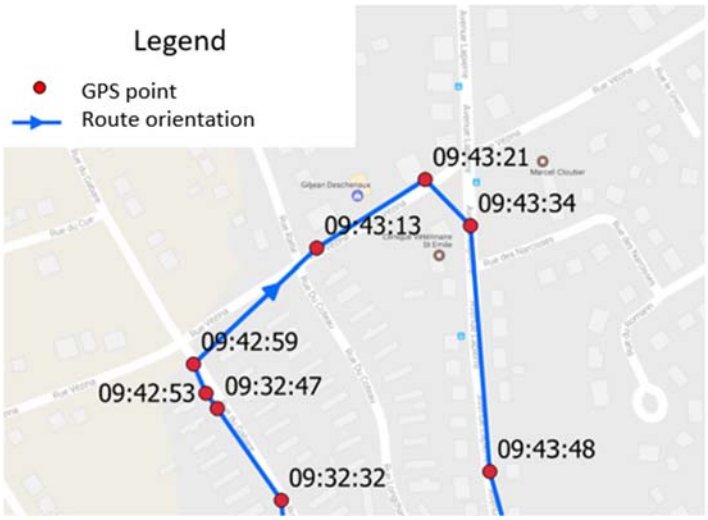

Figure 2. Determining the direction of a route

Identification of the precise path of each trip

The second step is to identify which segment was actually traversed. To this end, we created a buffer around each trip (Figure 3.a). This buffer is fixed according to the recording equipment used (25 meters for PDA and 15 meters for ELDs). We then considered all the road segments belonging to the created buffer zone. A sub-network is then defined for each trip (Figure 3.b). Subsequently, we projected the first recorded GPS point as well as the last onto the closest road segments to the previously defined sub-network. The closest junction nodes are then defined as the starting and ending points of the path (Figure 3.c). Next, we identify the GPS points that touch a single road segment when considering its buffer; these points are then assigned to their segment as no further decision needs to be made about them (Figure 3.d). Subsequently, we computed the path between the start and end nodes passing through the GPS points that are already assigned to their segments in the subnetwork (Figure 3.e). The Dijkstra algorithm is used to determine the shortest path. Having accurately identified the route and segments traveled, it is possible to make a final assignment of unassigned GPS points to their nearest segment without error (Figure 3.f).

a) The buffer zone

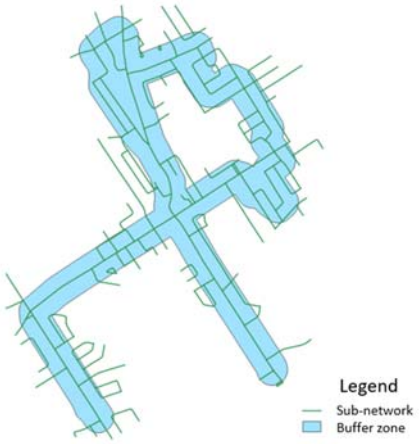

b) The related sub-network

c) Starting and ending nodes of the path

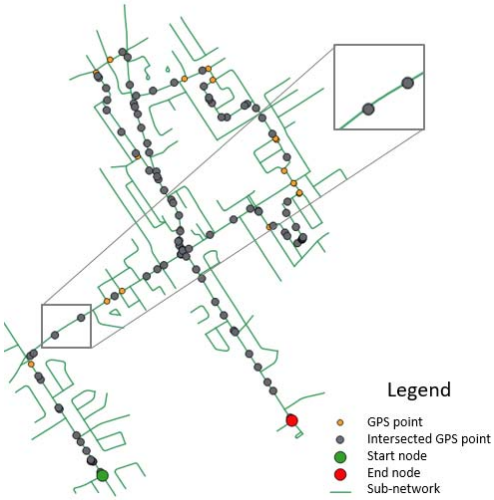

d) Points related to a single segment

e) Path calculation

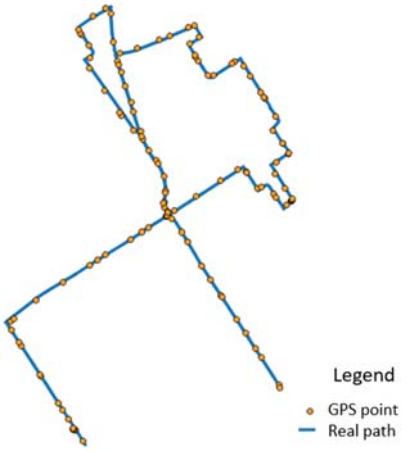

f) Assignment of the remaining points

Figure 3. Determining the precise path of each route

This step ends by determining the direction of movement on each segment. To do this, we use the attributes *fromnode* (start node) and *tonode* (end node) of the road segments added when creating the topology of the network. We identify the direction of the segments with respect to the directions of the road segments as created in the topology. Figure 4 illustrates an example of a path from *a* to *d* composed of three segments [*a*, *b*], [*b*, *c*] and [*c*, *d*]. According to the *fromnode* (F) and *tonode* (T) attributes of each segment, the segments were crossed in the (TF) direction for the segment [*a*, *b*], in the (TF) direction on the segment [*b*, *c*] and in the (FT) direction on the segment [*c*, *d*]. Thus, the GPS points associated with each trip will be assigned to the right direction with respect to their segment.

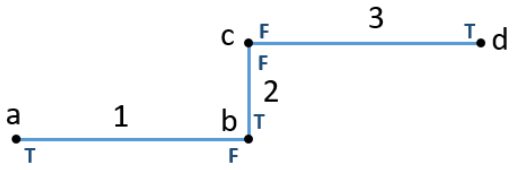

Figure 4. Determining the direction of each road segment

3.4 Average speeds calculation by time slots

The objective of this step is to compute the average speed on each segment according to the desired aggregation of time and days. We first sort each GPS observation by date, hour, and quarter of an hour. We assigned values from 0 to 6 on all days of the week (0 for Sunday and 6 for Saturday), 0 to 23 for hours, and 0 to 3 for a quarter-hour (0 for 0 to 15, minutes, 1 for 15 to 30 minutes, 2 for 30 to 45 minutes, 3 for 45 to 60 minutes). This allows one to filter the GPS points in increments of 15 minutes and filter the related databases. Then, for a given segment, we calculated the average speed of all GPS points recorded in the same time interval and having the same direction of movement. Note that these GPS points can belong to several routes with different origins and destinations as long as they traverse this segment. The relevant databases are then updated. Thus, the data treatment of a new Monday will update the databases *Monday* as well as the database *Week*.

Various types of data aggregations can be performed, by week, by time interval, by month, by season, and so on. Having the nominative information on each road segment (length, orientation, speed limit), we can estimate a congestion coefficient as the ratio between the computed average speed and the speed limit. For a given segment, we can obtain its congestion coefficient for each 15-minute interval,

from Monday to Sunday, and display this information in the form of a spreadsheet, an XML file or to visualize it with the help of a road map by coloring the segments according to the observed congestion coefficient.

Two examples of the observed coefficients plotted over the map of Quebec City are shown in Figure 5.

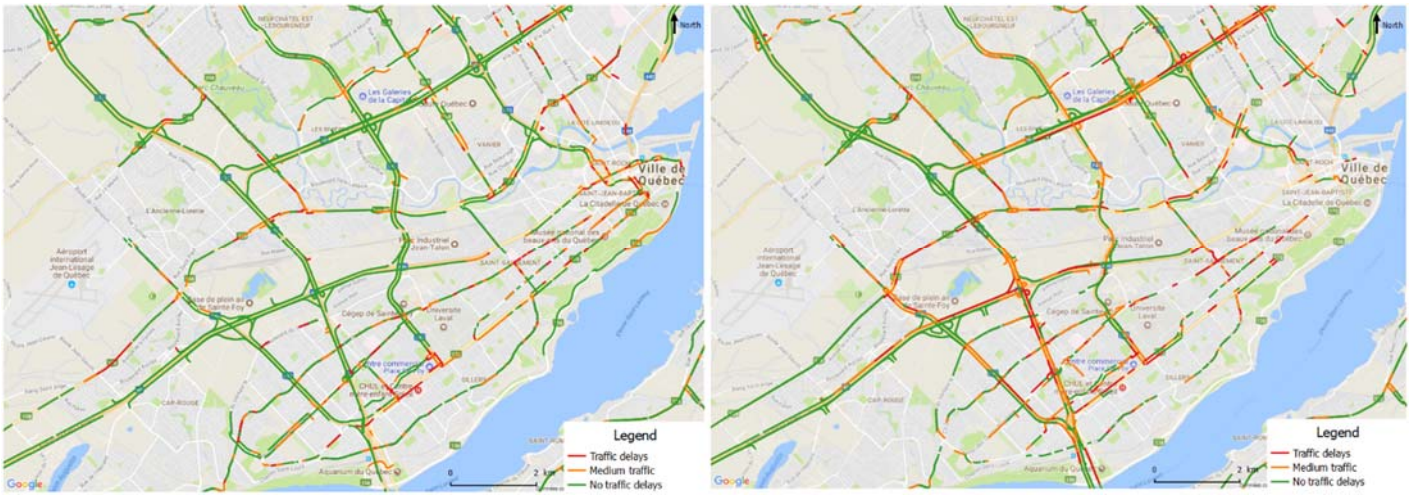

a) Friday 9h45 b) Friday 16h30

Figure 5. Two examples of the visualization of the congestion coefficients

3.5 Route duration according to road congestion

A given route can be considered as an ordered set $I = \{s_1, s_2, ..., s_n\}$ of n segments s_i such that the head of the segment s_1 is the starting point of the route and the tail of segment s_n is the destination of the route. The tail of segment s_i corresponds to the head of the segment s_{i+1} for $i = 1, ..., n\text{-}1$. We define a_i and b_i, $i = 1, ..., n$, as the time of entry and exit of segment s_i, respectively. Initially only a_1 is known, that is, the departure time of the route. Although we can generalize the calculations for any trip I, we will assume a route performed by a delivery truck, such that the route starts and ends at a depot. Hence, the head of s_1 and the tail of s_n correspond to the depot. This route of n segments is used to serve m customers, $m < n$. In order to simplify the notation, we will assume that each customer is located at the end of a segment s_i and that its service time is δ_i units. If the end of a segment does not correspond to a customer, the service time associated with the segment is simply $\delta_i = 0$.

To each segment s_i is associated a length l_i and a nominal speed v_i (set to the speed limit of this segment). The nominal duration of route I, denoted $D(I)$, is calculated as follows:

$$D(I) = \sum_{i=1}^{n} \left({}^{l_i}/_{v_i} \right).$$

The nominal duration of a route is the driving time if the vehicle is traveling at full speed and the stopping times (service times and traffic lights) are neglected. The nominal duration is independent of the starting time of the route, the day, and the congestion.

Using the information contained in the database, each segment s_i has an observed speed $\bar{v}_i^t$ when entered in period t. Thus, if segment s_i is entered at the time $t = a_i$ with a speed $\bar{v}_i^t$, the travel time will be ${}^{l_i}/_{\bar{v}_i^t}$. The congestion coefficient of segment s_i during the time interval t is $\varepsilon_i^t = {}^{\bar{v}_i^t}/_{v_i}$ where $\bar{v}_i^t$ is the average observed speed of segment s_i during time interval t and v_i is the nominal speed. We define $\bar{d}(i)$ as the time required to traverse segment s_i for a given start time and excluding the service time. The calculation of the duration of a route begins with the first segment which is entered at time a_1 and left at time b_1.

$$\bar{d}(1) = {}^{l_1}/_{\bar{v}_1^{a_1}}$$

$$b_1 = a_1 + \bar{d}(1) + \delta_1.$$

Then, recursively from $i = 2$ to n:

$$a_i = b_{i-1}$$

$$\bar{d}(i) = {}^{l_i}/_{\bar{v}_i^{a_i}}$$

$$b_i = a_i + \bar{d}(i) + \delta_i.$$

Then $\overline{D}(I) = b_n$ denotes the time required to travel and serve the customers of route I when it starts at time a_i with the observed speed as a function of the time where each segment is crossed. The driving time, without service times, is denoted $\overline{\overline{D}}$:

$$\overline{\overline{D}} = \overline{D}(I) - \sum_{i=1}^{n} \delta_i.$$

This calculation method assumes that for a given time interval, only one speed is associated with each segment. This assumption is not very restrictive considering that the road segments are relatively short and that the time to travel them is significantly smaller than the considered time interval of 15 minutes. With such a time interval, in practice, a segment could only have two different speeds if it overlapped exactly two time slots. The preceding formulas could then be easily adapted.

Information propagation

When evaluating a route *I*, it is possible that some segments for a given time *t* do not have an observed speed $\bar{v}_i^t$ in the database. Using the speed limit to these segments would neglect information available on neighboring segments. Thus, in the absence of an observed speed, we propagate the information available on the adjacent segments of the route according to the time period *t* when the segment will be traversed. Thus a congestion coefficient ε_i^t will be calculated as soon as a segment s_i with no observed speed is found between two incoming and outgoing segments s_{e_i} and s_{s_j} having congestion information available. The congestion coefficient will be calculated by averaging the coefficients of the incoming and outgoing adjacent segments as $\varepsilon_i^t = (\frac{\sum_{j=1}^{n} \varepsilon_{e_j}^t + \sum_{j=1}^{k} \varepsilon_{s_j}^t}{n+k})$ (see Figure 6). Only adjacent segments with information are considered in the calculation.

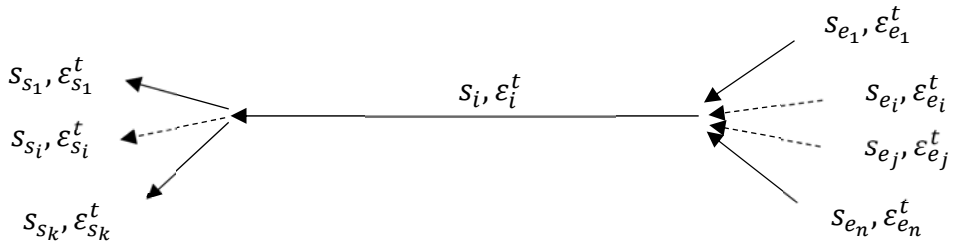

Figure 6: Information propagation on segment s_i

4. Case study

In this section we present different congestion analyses on the data collected from our industrial partner. First, we show that the developed method allows us to analyze how the congestion impacts the delivery sectors of the company. Subsequently, a set of routes will be analyzed in detail to validate the method developed with the actual data. Finally, we show how information can be used to determine the best start times to minimize the length of the delivery routes. This has important implications on fuel consumption and GHG emissions, as demonstrated at the end of this section.

4.1 Calculation of sectorial congestion

We use the data collected from our partner to determine the congestion that faces its vehicles in their different delivery sectors. Figure 7 details the Quebec City region according to the nine distribution sectors used by the company. For each sector, we analyzed all the road segments with traffic information. For each 15-minute time slot and for each sector, we calculated the average congestion ratio as the average of the segment congestion ratios for which we have an observation. Globally 27,945 road segments share 3,450,265 observations taken between March 06, 2015 and March 20, 2017.

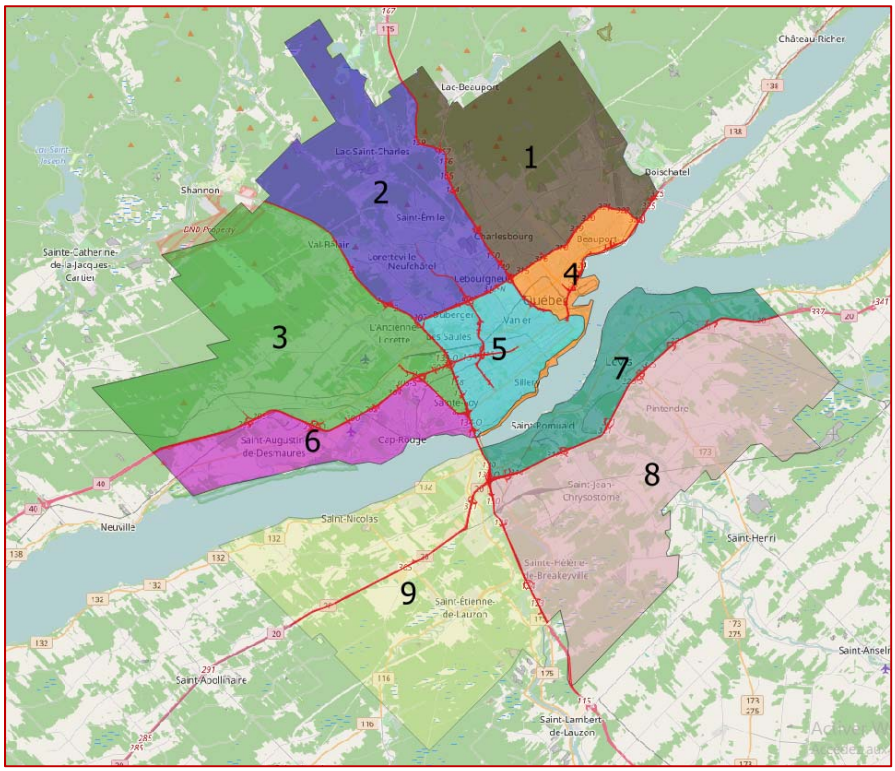

Figure 7. The nine distribution sectors in the Quebec City region

Figure 8 shows the evolution of congestion ratio on 52 intervals of 15 minutes ranging from 6:00 to 19:00. Sectors 1, 4, 5 and 6 are the most congested. Sector 4 shows the worst average congestion factor (0.49) in the interval between 13h30 and 13h44. This sector is the downtown neighborhood of Quebec, which includes the touristic areas as well as the parliament, and the main government departments of Quebec. This information is sorted differently in Table 1, which breaks the 52-time slots into five subsets: before morning traffic, morning traffic, midday, end-of-day traffic, and end of the day. The most congested time slot is from 7:30 to 10:15 with an average ratio of 0.59. Between 10h15 and

13h44, sector 4 shows the worst congestion ratio with 0.51. The column Global Average reports the results for each sector over the 52-time slots. The global speed observed for all the segments corresponds to 65% of the speed limit.

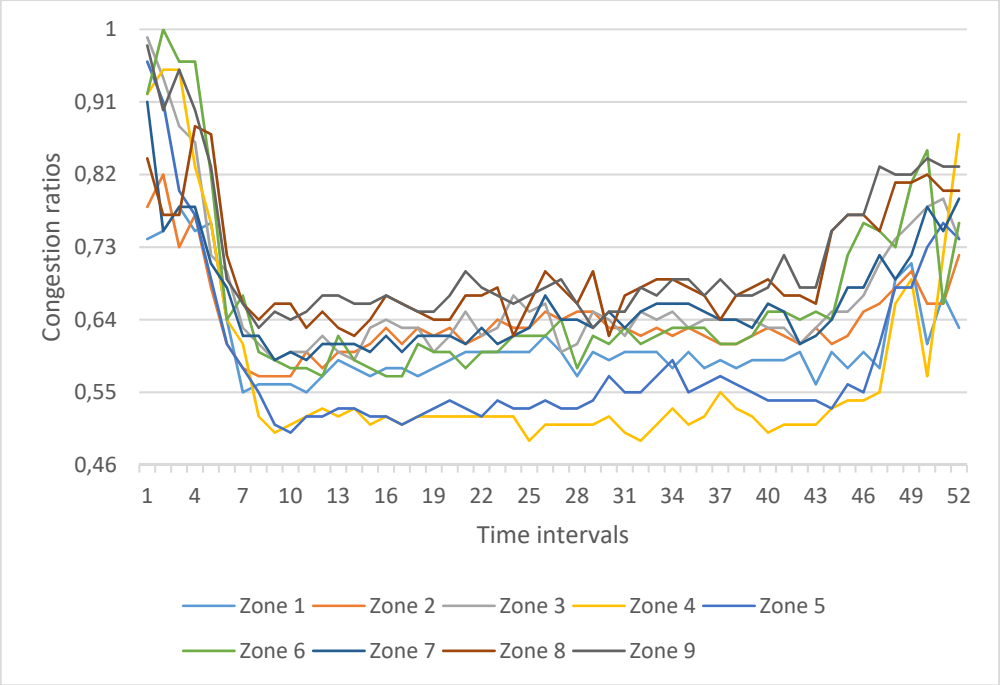

Figure 8. Evolution of congestion ratios

Table 1. Sectorial congestion factor

Sectors	6h00 7h29	7h30 10h14	10h15 13h44	13h45 17h29	17h30 18h59	Global Average
1	0.74	0.57	0.59	0.59	0.65	0.61
2	0.73	0.59	0.63	0.62	0.68	0.64
3	0.85	0.61	0.63	0.64	0.75	0.67
4	0.84	0.53	0.51	0.52	0.68	**0.57**
5	0.79	0.53	0.54	0.55	0.70	**0.59**
6	0.88	0.59	0.61	0.64	0.76	0.67
7	0.77	0.61	0.63	0.65	0.74	0.66
8	0.81	0.65	0.66	0.69	0.80	0.70
9	0.88	0.66	0.67	0.70	0.83	0.72
Average	0.81	**0.59**	0.61	0.62	0.73	0.65

4.2 Analysis of delivery routes

In this section we analyze in detail a representative set of 27 routes performed by our partner, three by delivery sector. Our analyzes are based on the service time as well as the driving time. In Table 2, the *Planned Service Time* column is the customer's standard service and installation time as determined by the company. The *Observed Service Time* is the actual time observed in the routes, obtained by recalculating GSP data allowing us to know when a vehicle stops at a customer's coordinates and when it departs this location. This first analysis shows a tendency of the company to overestimate installation times as the planned time for the 27 routes is 162h01 and the real time was 146h17, an overestimation of 944 minutes (on average 35 minutes per route). This shows that the software used by our partner largely ignores traffic and compensates this discrepancy by increasing service time. As we will observe later, this has negative effects on the creation of efficient vehicle routes.

In terms of driving time, the *Planned Driving Time* is the estimated time of the current routing software that does not take into account traffic congestion. This is the time given to the drivers on their bill of delivery. The *Observed Driving Time* was obtained by analyzing the GPS points of each route and determining the actual driving time, which excludes service times, the length of the lunch break and the associated movements. Finally, the *Estimated Driving Time* is our estimation for the timing of each route by taking into account traffic conditions as presented in the previous sections. To this end, we used exactly the same segments and determined the travel times according to the congestion ratio associated with the time interval when this segment was traversed. In order to manage the time properly we used the same installation and pause times to accurately reproduce the routes and determine their duration according to the congestion information present in our traffic database.

Table 2. Detailed analysis of the delivery routes

Routes	Service time		Difference	Driving time			Difference
	Planned	**Observed**	(minutes)	**Planned**	**Observed**	**Estimated**	(minutes)
1	5 h 59	6 h 46	47	0 h 59	1 h 44	1 h 35	-9
2	5 h 18	4 h 11	-67	0 h 12	1 h 03	1 h 05	2
3	5 h 39	5 h 07	-29	0 h 47	1 h 11	1 h 27	16
4	5 h 42	5 h 13	-29	0 h 36	0 h 58	1 h 10	12
5	5 h 19	4 h 44	-35	0 h 56	1 h 14	1 h 21	7
6	6 h 23	7 h 54	91	0 h 42	1 h 11	1 h 15	4
7	7 h 02	6 h 03	-59	0 h 41	1 h 15	1 h 18	3
8	7 h 02	5 h 48	-74	0 h 49	1 h 11	1 h 10	-1
9	6 h 09	6 h 09	0	1 h 24	1 h 37	1 h 39	2
10	6 h 13	6 h 34	20	0 h 56	1 h 43	1 h 42	-1
11	7 h 19	6 h 07	-72	0 h 42	1 h 14	1 h 13	-1
12	6 h 17	7 h 57	100	0 h 51	2 h 01	1 h 42	-19
13	6 h 08	8 h 20	132	0 h 36	1 h 46	1 h 29	-17
14	5 h 09	5 h 30	21	0 h 45	1 h 43	1 h 49	6
15	6 h 22	5 h 01	-81	0 h 58	1 h 42	1 h 39	-3
16	4 h 58	5 h 13	15	0 h 56	1 h 26	1 h 15	-11
17	7 h 45	5 h 03	-162	1 h 08	2 h 12	2 h 11	-1
18	5 h 19	3 h 39	100	1 h 16	1 h 23	1 h 30	7
19	7 h 48	5 h 18	-150	0 h 35	2 h 37	2 h 37	0
20	4 h 55	4 h 15	-40	1 h 42	1 h 51	1 h 42	-9
21	4 h 37	3 h 36	-61	1 h 37	1 h 57	2 h 07	10
22	4 h 32	3 h 50	-42	0 h 54	1 h 34	1 h 39	5
23	5 h 57	4 h 13	-104	1 h 19	2 h 29	2 h 19	-10
24	5 h 14	4 h 26	-48	1 h 22	1 h 28	1 h 30	2
25	6 h 59	6 h 24	-35	0 h 42	1 h 32	1 h 17	-15
26	4 h 54	4 h 11	-43	1 h 17	2 h 15	2 h 27	12
27	7 h 05	4 h 46	-139	1 h 35	2 h 00	2 h 14	14
Total	**162h01**	**146h17**	**-944**	**26h17**	**44h30**	**44h32**	**5**

The results in Table 2 show that the observed driving times are consistently higher than the planned times with an observed time of 44:30 compared to a planned time of 26:17. Our estimated driving times are much closer to the observed times with an estimated total of 44:32 which is a 5 minute difference from the total actual driving time for the 27 routes. This result confirms that the developed method provides an excellent estimate of actual travel times, which is much more accurate than the software currently in place at the company.

4.3 Determining the best departure times

Since the length of a delivery route depends on the congestion, it is influenced by the departure time. For each route, we recalculated the driving times for the departure time that was chosen by the company as well as for potential departures between 6:00 and 13:00, for time intervals of 15 minutes. Table 3 presents for each route its current departure time, the optimal and the worst departure times. Thus, for Route 1, the best departure time would be to leave the depot at 12:00 with a route length estimated at 1h12 which is 22 minutes quicker than starting at 7:35. The worst departure time of Route 1 is at 8:00 with an estimated duration of 1:35, one minute longer than the time associated with the current time of departure at 7:35. Table 3 shows that for the routes studied, using the optimal departure time for each route would reduce the total delivery duration from 44:32 to 32:27, i.e., a reduction in driving time of 12 hours and 5 minutes, which corresponds to 27%.

Unfortunately, because of the associated return times, some of these routes are not acceptable to customers nor to the company. Indeed, the return of Route 1 at 21:12 is not applicable due to customer service restrictions. Table 4 then reproduces the same analysis, but imposing departure times after 07:00 and return times to the depot before 19:00. This time interval is realistic and minimizes the impact on customer service. Even if the time savings are lower, a reduction in travel time of 9:50 is observed, or 22%. Considering two installers per vehicle, each costing the company about 21 $/h, this reduction corresponds to a saving of 413 $ (9.83 × 21 × 2). If this 27-routes saving is considered to an average of 40 routes per day, this totals to savings of 612 $ per day.

Table 3. Departure time analysis

Routes	Departure time		Optimal departure time					Worst departure time		
	Current					Improvement				
	Time	Length	Time	Length	Return	Length	%	Time	Length	Return
1	07:35	1 h 34	12:00	1 h 12	21:12	0 h 22	24	08:00	1 h 35	17:35
2	07:34	1 h 05	06:30	0 h 59	11:53	0 h 06	10	08:00	1 h 07	13:31
3	07:04	1 h 27	12:00	1 h 08	18:24	0 h 19	22	07:00	1 h 29	13:45
4	07:38	1 h 10	12:00	0 h 47	18:37	0 h 23	33	07:30	1 h 17	14:37
5	07:46	1 h 21	06:00	0 h 55	11:54	0 h 25	32	07:46	1 h 21	14:06
6	07:38	1 h 15	12:00	0 h 52	21:39	0 h 23	31	07:38	1 h 15	17:40
7	07:42	1 h 18	11:00	0 h 56	19:21	0 h 21	28	07:42	1 h 18	16:25
8	07:34	1 h 10	12:00	0 h 55	19:43	0 h 14	21	08:30	1 h 11	16:29
9	07:31	1 h 39	11:00	1 h 10	19:16	0 h 28	29	07:30	1 h 41	16:16
10	07:32	1 h 42	12:00	1 h 08	20:45	0 h 33	33	07:32	1 h 42	16:52
11	07:51	1 h 13	06:00	0 h 47	13:35	0 h 25	35	07:51	1 h 13	15:52
12	07:03	1 h 42	12:00	1 h 20	22:14	0 h 21	21	09:00	1 h 50	19:44
13	07:38	1 h 29	12:00	0 h 50	22:02	0 h 38	43	07:38	1 h 29	18:19
14	07:31	1 h 49	11:00	1 h 00	17:55	0 h 48	45	07:31	1 h 49	15:15
15	07:50	1 h 39	11:30	1 h 18	19:19	0 h 20	20	07:30	1 h 44	15:45
16	07:34	1 h 15	11:00	0 h 57	17:10	0 h 17	23	07:34	1 h 15	14:02
17	07:10	2 h 11	12:00	1 h 39	20:40	0 h 32	24	07:30	2 h 12	16:44
18	07:36	1 h 30	12:00	1 h 03	16:45	0 h 26	30	07:36	1 h 30	12:48
19	07:19	2 h 37	11:30	1 h 42	20:13	0 h 55	35	07:19	2 h 37	16:58
20	08:05	1 h 42	12:00	1 h 25	18:53	0 h 17	17	07:00	1 h 34	14:18
21	07:42	2 h 07	12:00	1 h 33	17:09	0 h 33	27	07:42	2 h 07	13:25
22	07:34	1 h 39	11:30	1 h 13	16:45	0 h 26	26	07:30	1 h 45	13:17
23	07:42	2 h 19	06:00	1 h 43	13:00	0 h 35	26	07:30	2 h 29	15:16
24	07:34	1 h 30	11:00	1 h 05	16:56	0 h 24	27	07:34	1 h 30	13:55
25	07:06	1 h 17	12:00	1 h 02	20:59	0 h 14	19	08:00	1 h 28	17:25
26	07:44	2 h 27	12:00	1 h 44	18:10	0 h 42	29	07:44	2 h 27	14:37
27	07:32	2 h 14	11:30	1 h 50	19:15	0 h 23	17	07:30	2 h 15	15:39
Total		**44h32**		**32h27**		**12h05**	**27**		**45h21**	

Table 4. Routes length with departure times after 7:00 and return time before 19:00

Routes	Actual departure		Best feasible departure			Improvement	
	Time	Length	Time	Length	Return	Length	%
1	07:35	1:34	09:00	1:22	18:22	0:22	24
2	07:34	1:05	09:00	1:00	14:24	0:05	8
3	07:04	1:27	12:00	1:08	18:24	0:19	22
4	07:38	1:10	12:00	0:47	18:37	0:23	33
5	07:46	1:21	10:30	1:00	16:29	0:21	26
6	07:38	1:15	09:00	1:03	18:50	0:12	17
7	07:42	1:18	07:30	1:03	15:58	0:21	28
8	07:34	1:10	11:00	0:59	18:47	0:14	21
9	07:31	1:39	10:30	1:15	18:50	0:28	29
10	07:32	1:42	09:30	1:13	18:20	0:33	33
11	07:51	1:13	11:00	0:48	18:35	0:25	34
12	07:03	1:42	07:03	1:42	17:38	0:00	0
13	07:38	1:29	07:00	1:07	17:19	0:25	29
14	07:31	1:49	11:00	1:00	17:55	0:48	45
15	07:50	1:39	10:30	1:30	18:31	0:20	20
16	07:34	1:15	11:00	0:57	17:10	0:17	23
17	07:10	2:11	10:00	1:46	18:47	0:26	20
18	07:36	1:30	12:00	1:03	16:45	0:26	30
19	07:19	2: 37	09:30	1:52	18:23	0:51	32
20	08:05	1:42	12:00	1:25	18:53	0:17	17
21	07:42	2:07	12:00	1:33	17:09	0:33	27
22	07:34	1:39	11:30	1:13	16:45	0:26	26
23	07:42	2:19	11:00	1:49	18:06	0:35	25
24	07:34	1:30	11:00	1:05	16:56	0:24	27
25	07:06	1:17	09:30	1:10	18:37	0:06	9
26	07:44	2:27	12:00	1:44	18:10	0:42	29
27	07:32	2:14	11:00	1:56	18:50	0:23	17
Total		**44:32**		**34:42**		**9:50**	**22**

4.4 Reduction of CO_2 equivalent emissions

In this section we evaluate GHG emission savings achieved by reducing the duration of delivery routes. Since the distances traveled are exactly the same, only the 9:50 travel time reduction from Table 4 has to be converted into CO_2 *equivalent* emissions, denoted CO_2 *e*. It is impossible to determine with certainty how these 9:50 reduction was achieved (i.e., was the truck stuck in traffic, or driving slower in some segments, or constantly accelerating and breaking). For this reason we used different methods to quantify the reduction of emissions. The first one assumes that the vehicle engine is idle during the time saved. This estimate is actually a lower bound on the emission reductions. According to Natural Resources Canada (2017), light-duty vehicle consumption is estimated at 1.80 l/60 min. One liter of diesel generates 2.60 kg of CO_2 and other gases that correspond to, under a common measure, to 2.79 kg CO_2 *e* (MERN, 2014). It can be estimated that an engine running idle during for 590 minutes generates 49.38 kg CO_2 *e* (590 minutes × 1.80 l/60min × 2.79 kg CO_2 *e*/l). Hence, we estimate that the minimum saving is that we avoided the engine to be idle for 9:50 which would reduce emissions in 49.38 kg CO_2 *e*.

The second method is based on the average speed of the routes. First, we calculate the precise distance of the route (in meters). From this distance and the driving time of the route (relative to its departure time), we deduce its average speed (V_1). We proceed in the same way to calculate the average speed associated with the optimal departure time from Table 4 (V_2). We then use the *Comprehensive Modal Emissions Model* (CMEM, 3.01) to calculate fuel consumption and CO_2 *e* emissions for these two routes (Barth and Boriboonsomsin, 2008, 2009). The difference in the amount of CO_2 *e* emitted by the routes for two departure times (the actual departure time and the optimal one) represents the reduction of CO_2 *e* emissions associated with the time saved.

Route 1 will be used as an example. The road distance is 45.588 km and it was traveled in 94.5 minutes (Table 4) for an average speed of 28.9 km/h. For these parameters, the CMEM provides a consumption of 11.14 liters (24.4 l/100 km) and emissions of 31.12 kg CO_2 *e*. A departure at 9:00 provides an 82-minute route, which corresponds to an average driving speed of 33.4 km/h. The CMEM provides a fuel consumption of 10.10 liters (22.15 l/100 km) and emissions of 28.18 kg CO_2 *e*. The reduction in emissions for Route 1 only is therefore 2.94 kg CO_2 *e*.

Overall, the 27 routes have a length of 1 717 km and the application of the CMEM with the actual departure times leads to an average consumption of 20.60 l/100 km for a total consumption of 353.7 l. The application of CMEM on these routes with their optimal departure times leads to an average consumption of 18.76 l/100 km. This difference of 1.84 l/100 km yields, for all the routes, a total reduction of 31.59 liters and of 88.13 kg CO_2 *e*. This corresponds to an average reduction of 9.6%. Hence, this realistic estimation shows savings that are almost double those of the idle engine method.

For the roads analyzed, the CMEM reports consumptions between 18.76 and 20.60 l/100 km, for an average consumption of 19.68 l/100 km. It is good to put these numbers in perspective with other sources. In comparison, HinoCanada, which manufactures the HINO D195 vehicles used by our partner, advertises a consumption of 22 l/100 km. The transportation managers of our partner base their estimates on a consumption of 25 l/100 km. The last two rows of Table 5 therefore project the emission reductions proportionally according to these consumption rates. Considering that our partner performs an average of 10 500 delivery routes per year, we can estimate that a better management of departure times could save between 12,285 and 15,606 liters of diesel per year, i.e., between 38 and 43 tons of CO_2 *e* per year.

Table 5. Reduction in fuel consumption and GHG emissions

Calculation method	Consumption in liters per 100 km	Reduction for 27 routes		Projected reduction for 10 500 routes	
		liters	CO_2 *e*(kg)	liters	CO_2 *e* (t)
Idle	1.80	17.70	49.38	6 833	19.20
CMEM	[18.76 ; 20.60]	31.59	88.13	12 285	34.27
HinoCanada	22.0			13 733	38.31
Partner estimates	25.0			15 606	43.53

5. Conclusions

Most vehicle routing algorithms consider constant speed. In practice, speed is affected by several variables including, among others, the state of road traffic at different times of the day. The time-dependent vehicle routing problem (TDVRP) allows us to consider some congestion issues. Nevertheless, the TDVRP is mostly based on simulated congestion data. In this article we have described and validated a detailed methodology that allows to establish precise maps of traffic congestion as a function of time from GPS observations. We have demonstrated the precision of the methodology developed by comparing our estimates with the routes performed by our industrial partner. This information can be used to optimize the departure time of vehicles according to congestion and thus reduce driving times of drivers. This dynamic management of departure times allows reductions in the order of 22% of travel times. These reductions translate into savings of between 12,285 and 15,606 liters of diesel per year, or between 38 and 43 tons of CO_2 *e* per year.

Acknowledgments

This research was partly supported by grants 2014-05764 and 017633 from the Natural Sciences and Engineering Research Council of Canada (NSERC) and by the *Centre d'Innovation en Logistique et Chaîne d'Approvisionnement Durable* (CILCAD). The CILCAD receives financial support from the Green Fund under Priority 15.2 of the 2013-2020 Action Plan on Climate Change, a priority implemented by *Transition Énergétique Québec* (TEQ). We also thank Logix Operations inc. and an important wholesaler partner in Quebec City for providing us with real data. This support is highly appreciated.

References

Barth, M., Boriboonsomsin, K., (2008). Real-world CO_2 impacts of traffic congestion. *Transportation Research Record: Journal of the Transportation Research Board*, 2058, 163-171.

Barth, M., Boriboonsomsin, K., (2009). Energy and emissions impacts of a freeway-based dynamic eco-driving system. *Transportation Research Part D: Transport and Environment*, 14, 400-410.

Bektas T., Laporte, G., (2011). The pollution-routing problem. *Transportations Research Part B*, 45, 1232-1250.

Bernstein, D. and Kornhauser, A., (1996). *An introduction to map matching for personal navigation assistants*. New Jersey TIDE Center.

Coelho, L. C., Cordeau, J.-F., Laporte, G., (2014). Thirty years of inventory-routing. *Transportation Science*, 48, 1-19.

Coelho, L. C., Gagliardi, J.-P., Renaud, J., Ruiz A., (2016). Solving the vehicle routing problem with lunch break arising in the furniture delivery industry. *Journal of the Operational Research Society*, 67, 743-751.

Comprehensive Modal Emission Model and NCHRP 25-11 Vehicle Emission Database, University of California, Riverside, College of Engineering – *Center for Environmental Research & Technology*. CMEM Version 3.01.

Cordeau, J.-F., Laporte, G., (2005). Tabu search heuristics for the vehicle routing problem. In *Metaheuristic Optimization via Memory and Evolution. Tabu search and scatter search*. Kluwer Academic Publishers, 145-164.

Gagliardi, J.-P., Renaud J., Ruiz A., (2013). Solving a real vehicle routing problem in the furniture and electronics industries. *Document de travail CIRRELT* 2013-035.

Gendreau, M., Ghiani G., Guerriero E., (2015). Time-dependent routing problems: A review. *Computers & Operations Research*, 64, 189-197.

Gendreau, M., Laporte G., Potvin, J.-Y., (2002). Metaheuristics for the capacitated VRP. In *The Vehicle Routing Problem*, P. Toth and D. Vigo (eds), SIAM Monographs on Discrete Mathematics and Applications, Philadelphia, 129-154.

Greenfeld, J.S., (2002). Matching GPS observations to locations on a digital map. In *Proceedings of the 81st Annual Meeting of the Transportation Research Board*, January, Washington D.C.

Honey, S.K., Zavoli, W.B., Milnes, K.A., Phillips, A.C., White, M.S., Loughmiller, G.E., (1989), Vehicle navigational system and method, United States Patent No., 4796191.

Ichoua, S., Gendreau, M., Potvin, J.-Y., (2006). Exploiting knowledge about future demands for real-time vehicle dispatching, *Transportation Science*, 40, 211-225.

Koç Ç, Bektaş T., Jabali O., Laporte G., (2016). Thirty years of heterogeneous vehicle routing, *European Journal of Operational Research*, 249, 1-21.

Kok, A. L., Hans E. W., Schutten, J.M.J., (2012). Vehicle routing under time-dependent travel times: The impact of congestion avoidance, *European Journal of Operational Research*, 39, 910-918.

Laporte, G., (2009). Fifty years of vehicle routing. *Transportation Science*, 43, 408-416.

Li, Z., Chen, W., (2005). A new approach to map-matching and parameter correcting for vehicle navigation system in the area of shadow of GPS signal. In: *IEEE Conference on Intelligent Transportation Systems*, ITSC, 425–430.

Ministère de l'Énergie et des Ressources Naturelles (MERN), 2014. Bureau de l'efficacité et de l'innovation énergétique, *Facteurs d'émissions et de conversion*, Gouvernement du Québec.

Ochieng, W.Y., Quddus, M.A., Noland, R.B., (2004). Map-matching in complex urban road networks. *Brazilian Journal of Cartography* (*Revista Brasileira de Cartografia*), 55, 1–18.

ORMS Today, Vehicle routing: Driving transformation. February, 43, 2016.

Pillac, V., Gendreau, M., Guéret, C., Medaglia, A. L., (2013). A review of dynamic vehicle routing problems. *European Journal of Operational Research*, 225, 1-11.

Potvin, J.-Y., (2009). Evolutionary algorithms for vehicle routing. *INFORMS Journal on Computing*, 21, 518-548.

Quddus, M.A., Ochieng, W. Y.,Zhao L., Noland R. B. (2003). A general map-matching algorithm for transport telematics applications. *GPS Solutions*, 7 (3), pp. 157-167.

Quddus, M.A., Ochieng, W. Y., Noland, R. B., (2007). Current map-matching algorithms for transport applications: State-of-the art and future research directions *Transportation Research Part E: Emerging technologies*, 15, 312-328.

Ritzinger, U., Puchinger J., Hartl, R. F., (2016). A survey on dynamic and stochastic vehicle routing problems, *International Journal of Production Research*, 25, 215-231.

Speranza, M. G., (2018), Trends in transportation and logistics. *European Journal of Operational Research*, 264, 830-836.

Wang B., Yang, Y., and Sun, Y., (2006). Research on high accurate and real-time map-matching algorithm in LBS, GMC'2006: *2006 Global Mobile Congress* – Papers, 258–262.

White, C., Bernstein, D., and Kornhauser, A., (2000). Some map matching algorithms for personal navigation assistants. *Transportation Research Part C: Emerging Technologies*, 8, 91-108.